

The Seebeck coefficient of the solid and liquid germanium

ERCAN BALIKCI*, REZA ABBASCHIAN

Materials Science and Engineering Department, University of Florida, Gainesville, Florida 32611, USA

E-mail: ercanbalikci@hotmail.com

The knowledge of the Seebeck coefficient of materials is essential in determining the actual solid/liquid interface temperature during the melt growth of crystals. In this study, the Seebeck coefficient of the solid and liquid germanium was measured employing the small ΔT technique. The Seebeck coefficient increased from $-107 \mu\text{V}/^\circ\text{C}$ at 857°C to $-54 \mu\text{V}/^\circ\text{C}$ at 931°C in the solid. However, an average constant value of $-0.6 \mu\text{V}/^\circ\text{C}$ was obtained in the liquid from 938 to 960°C , above which a value of $-18 \mu\text{V}/^\circ\text{C}$ was recorded. Also, when the liquid samples were cooled below the melting point, a melt supercooling was observed, which seemed to be larger with higher melt temperatures.

© 2005 Springer Science + Business Media, Inc.

1. Introduction

Crystal growth of many technologically important semiconductor materials has so far been carried out with a limited knowledge of the actual temperature of the solid/liquid (s/l) interface, which can easily supercool several tens of degrees depending on the crystal orientation, interface structure, and crystal growth velocity. Information on the real interface temperature can provide insight into the atomic attachment mechanism at the interface, hence the interface evolution mechanism, which affects the stability of the advancing interface in growing crystals.

Indirect and direct methods have been utilized to measure the interface temperature [1]. One generally employed indirect method to predict the interface temperature is the use of bulk temperature profile (furnace zone temperatures). However, many assumptions in these predictions do not yield an accurate interface temperature. Another indirect method is the application of heat waves, in which case the temperature of the interface is calculated by assuming a kinetic law and using the characteristics of applied and transmitted heat waves across the interface. This technique is also found to be very inconsistent and cannot be used during actual growth, as it interrupts the steady migration of the interface.

A way of measuring interface temperature directly is by means of a so-called fixed thermocouple method [1], in which the interface temperature is measured by thermocouples positioned at different heights in the solidifying liquid. As the interface reaches each thermocouple, the temperature is recorded at that location. However, thermocouples themselves distort the thermal field around them, in

turn, the temperature of the interface. Therefore, the real interface temperature still cannot be recorded accurately.

A non-intrusive Seebeck technique can also be exploited to determine the interface temperature directly. In this technique, there is no physical disturbance to the interface, and the technique utilizes the property of thermocouples [2], which are comprised of two dissimilar metal wires that are joined at both ends creating a loop with two junctions. When these junctions are held at different temperatures, the loop generates an electromotor force (voltage) that can be measured. Later, the temperature of a junction can be determined by use of the junction's Seebeck coefficient (S) that relates the change in the voltage to the change in the temperature at a junction, as will be described below. Thus, knowing S is a priory when determining a junction's temperature.

A solid/liquid interface can be considered as a junction whose temperature can be determined by exploiting the thermocouple theory. In this case, the solid and liquid represent two dissimilar materials. If the Seebeck coefficients of the solid and the liquid near the melting point are known, then the Seebeck coefficient of the s/l junction (interface), hence the interface temperature (T_{SL}), can be determined.

The Seebeck coefficient of materials is temperature dependent and can be determined in two ways: absolute and relative. Absolute Seebeck coefficient of materials, at a certain temperature T , can be determined directly by carrying out Thompson heat (σ_T) measurements [3] and then converting it to S_T , the Seebeck coefficient at that particular temperature, through

* Author to whom all correspondence should be addressed.

Equation 1.

$$S_T = \int_0^T (\sigma_T/T)dT \quad (1)$$

Alternatively, the Seebeck coefficient can be measured against a material with a well-known Seebeck coefficient by use of the small ΔT method. In this method, while one end of the material is kept at a constant temperature, the other end temperature is changed from T_1 to T_2 by a small amount ΔT , which is equal to $T_2 - T_1$ and is usually less than 10 degrees in practice. By measuring the voltage generated, E_T , due to the change in the temperature and using Equation 2, relative Seebeck coefficient can be found. As a different approach, the sample can be held in a temperature gradient, and both end temperatures can be changed by a small amount, again less than 10 degrees. Equation 2 is still applicable.

$$E_T = \int_{T_1}^{T_2} S_T dT \quad (2)$$

When measuring the Seebeck coefficient of a material, due to the wiring of the material to the voltage measuring instrument (e.g., voltmeter), junctions are created at the material-wire contacts, which can contribute to the generated voltage as noise that can be alleviated by keeping these junctions at an equal and constant temperature. A technique has been proposed and used [4–6] to determine the Seebeck coefficient with high accuracy due to creating two s/l interfaces, one of which is kept stationary and the other is translated. Since one interface is kept stationary at a known melting point, parasitic contributions due to temperature fluctuations are eliminated. This technique has been only used for low melting materials. Some other experimental configurations for determining the Seebeck coefficient or the interface temperature in different applications have also been reported, such as in determining the interface temperature of layered electronic structures [7–10].

Seebeck coefficient of germanium has been studied by holding germanium in a crucible and connecting voltage and temperature probes to both ends [11–16]. Reported Seebeck coefficient of solid has been found to decrease with decreasing temperature and had a negative value ($-50 \mu\text{V}/^\circ\text{C}$ at 938°C and $-450 \mu\text{V}/^\circ\text{C}$ at 100°C), which indicates an *n*-type material [17, 18], although Domenicali reported [15] similar values for *n*-type and *p*-type samples in a temperature range between 500°C and melting point of 938°C . He attributed similar values to the very low carrier concentration (less than 3×10^{15} ats./cc) in both types of samples. Ablova [19] observed that applied stress on solid germanium changes Seebeck readings appreciably, and it was attributed to the change in electron-hole ratio. In addition, although grain boundary contribution to the Seebeck signal is a concern [1, 20], it was reported [15] that poly or single crystal germanium produced similar values of the Seebeck coefficient. Unlike the varying Seebeck coefficient in the solid, a temperature independent value of about $-0.5 \mu\text{V}/^\circ\text{C}$ has been reported as the Seebeck coefficient of liquid germanium [11–16].

However, Glazov reported $-12 \mu\text{V}/^\circ\text{C}$ for liquid [21] at 977°C , although he also reported $-0.5 \mu\text{V}/^\circ\text{C}$ close to the melting point. In contrast, Ablova reported [19] a positive value of 15 to $20 \mu\text{V}/^\circ\text{C}$ for *p*-type liquid germanium at the melting point, although Domenicali again reported [15] similar values ($-0.5 \mu\text{V}/^\circ\text{C}$) for *n*-type and *p*-type liquids. Modeling calculations [22–24] predicted the Seebeck coefficient of liquid germanium between -1 and $-6 \mu\text{V}/^\circ\text{C}$. Higher Seebeck coefficient of liquid germanium was attributed to a semiconductor to metal transition upon melting. It has been reported [23, 25–28] that germanium has about 7 nearest neighbors in the liquid form, as opposed to 4 in the solid, which indicates a metallic transition. However, germanium still keeps its tetrahedral bond characteristics even in the liquid form [24–28], as metallic materials have 12 nearest neighbors.

Absolute Seebeck coefficient of the s/l interface is obtained after separately finding the solid and liquid Seebeck coefficients closer to the melting point and reported to be in the range of -90 to $-50 \mu\text{V}/^\circ\text{C}$ [15, 16]. Contrary to this, Ablova again reported a positive value, 15 to $25 \mu\text{V}/^\circ\text{C}$, at the fusion point of a germanium sample prepared from well defined *p*-type powders [19].

Results reported in this paper are a part of a NASA supported project exploring the morphological stability of s/l interfaces during crystal growth of antimony-doped germanium [29, 30]. The current paper presents the Seebeck measurements for the solid and liquid germanium along with some noteworthy observations seen in the superheated and supercooled liquids than can be imported for analysis of growing interfaces.

2. Experimental

Fig. 1 shows a schematic of the experimental unit, which consisted of a 3-zone vertical tubular furnace (1), a quartz tube (2), a monel pedestal rod (3), a graphite pedestal (4) housing the cold end probes (5), a quartz crucible (6) holding the germanium charge, and a graphite tube (7) housing the hot end probes (8). Two probes at each end (hot and cold) were constructed, one for measuring the temperature and the other for measuring the Seebeck voltage. The temperature probes at both ends were made of a special grade OMEGA brand Inconel sheathed *K*-type thermocouple, whereas the Seebeck (voltage) probes were made of a 1-mm diameter 99.9% purity copper wire. A molybdenum wire, voltage probe (99.999% purity) together with the copper probe was also used to cross check the voltage readings in two experiments. The voltage probes and the thermocouples were fed through a four-bore alumina sleeve, which was then inserted in the graphite pedestal (4) for cold end and graphite tube (7) for hot end as seen in Fig. 1. Four-bore alumina sleeve electrically insulated each probe from one another. A graphite glue paste was used between the graphite housings and tip of the probes to ensure a good electrical contact. The probes were 1 mm away from the outer surface of the housings; that is from the solid or liquid sample. Ultra high purity (99.999%) argon ran through the quartz

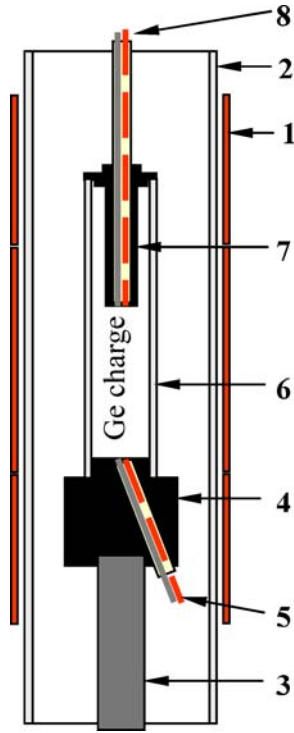


Figure 1 A schematic of the experimental set up used for the Seebeck voltage measurements, which consists of a 3-zone vertical tubular furnace (1), a quartz tube (2), a monel pedestal rod (3), a graphite pedestal (4) housing the cold end probes (5), a quartz crucible (6) holding the germanium charge, and a graphite tube (7) housing the hot end probes (8). Two probes on each end, cold (5) and hot (8), were constructed, one for measuring the temperature (solid line) and the other for measuring the Seebeck voltage (dashed line).

tube (2) to provide an inert environment. The data acquisition system consisted of a 12-bit OMEGA brand data acquisition card connected to a multiplexer with 100-gain, which gave a $24.42 \mu\text{V}$ resolution.

The experiments were performed using an *n*-type polycrystalline germanium of 99.9999% purity. The Seebeck voltage was measured at stabilized, constant temperatures with three different types of samples; completely solid, completely liquid, and partially solid/liquid. As listed in Table I, experiments #1, 2, 3 were carried out with completely solid samples, #4, 5, 6 with partially solid/liquid samples, and #7, 8, 9, 10 with initially completely liquid samples and later solidified

TABLE I Constant hot end temperatures (T_h) and range of the cold end temperatures (T_c) for various experiments conducted in this study. Experiments #1–#3 were conducted with fully solid Ge samples, #4–#6 with partially solid and partially liquid samples, and #7–#10 with initially fully liquid samples

#	T_h , C (± 1)	T_c , C (± 1)
1	907	900–854
2	915	901–875
3	935	933–917
4	944	937–912
5	959	934–880
6	961	934–875
7	963	951–898
8	985	967–929
9	988	970–927
10	1033	1000–906

to form a solid/liquid type sample. For the measurements, the hot end temperature (T_h) was kept constant while the cold end temperature (T_c) was reduced stepwise by decreasing the temperature of the lower zone of the vertical furnace. Both the hot and cold junctions could be kept constant within 2°C ($\pm 1^\circ\text{C}$). At each step, data collection lasted one hour after the temperature was reduced. The thermal stabilization of the system after temperature change took less than 10 min; still, only the data collected in the last 45 min were used in the calculations.

3. Results and discussions

An electrical wiring diagram, equivalent of the experimental set up in Fig. 1 is given in Fig. 2 to show better how the Seebeck voltage was generated in the system. As given by Equation 3, total voltage generated, E_T , can be written as an integral addition of each individual component in the system, namely the copper wire at both ends and the solid or liquid germanium sample.

$$E_T = \int_{T_{RT}}^{T_c} S_{Cu} dT + \int_{T_c}^{T_h} S_{Ge} dT + \int_{T_h}^{T_{RT}} S_{Cu} dT \quad (3)$$

where S_{Cu} is the Seebeck coefficient of copper, S_{Ge} is the Seebeck coefficient of the solid or liquid germanium, and temperatures on the integral limits are shown in Fig. 2. Evaluation of Equation 3 yields:

$$E_T = T_c S_{Cu-Ge} + T_h S_{Ge-Cu} \quad (4)$$

where $S_{Cu-Ge} = S_{Cu} - S_{Ge}$ at T_c and $S_{Ge-Cu} = S_{Ge} - S_{Cu}$ at T_h .

As T_h was kept constant during the experiments, change in the Seebeck voltage was generated only because of changing T_c . Hence, Equation 4 reduces to give the following:

$$\Delta E_T = \Delta T_c S_{Cu-Ge} \quad (5)$$

from which absolute Seebeck coefficient of the solid (S_S) or liquid (S_L) germanium can be found by using $S_{Cu-Ge} = S_{Cu} - S_{Ge}$, in which S_{Ge} represents either S_S or S_L depending on whether the sample is solid or liquid. Absolute Seebeck coefficient of copper (S_{Cu}) was extracted from the data table previously produced by Cusack and Kendal in 1958 [3]. Although Roberts [31, 32] also generated an absolute thermoelectric scale in 1981 and claimed to be more accurate than Cusack and Kendal's scale, we still used the earlier scale since it goes up to the high temperature range (1000°C) of our experiments. Roberts gives absolute Seebeck coefficient for copper at maximum 627°C , and at this temperature discrepancy between the two absolute scales is about 7%.

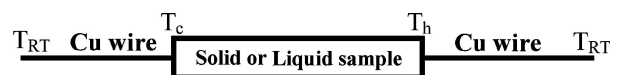


Figure 2 Schematic wiring diagram of the Seebeck voltage measurement set up shown in Fig. 1. T_{RT} = room temperature, T_c = cold end (junction) temperature, and T_h = hot end (junction) temperature.

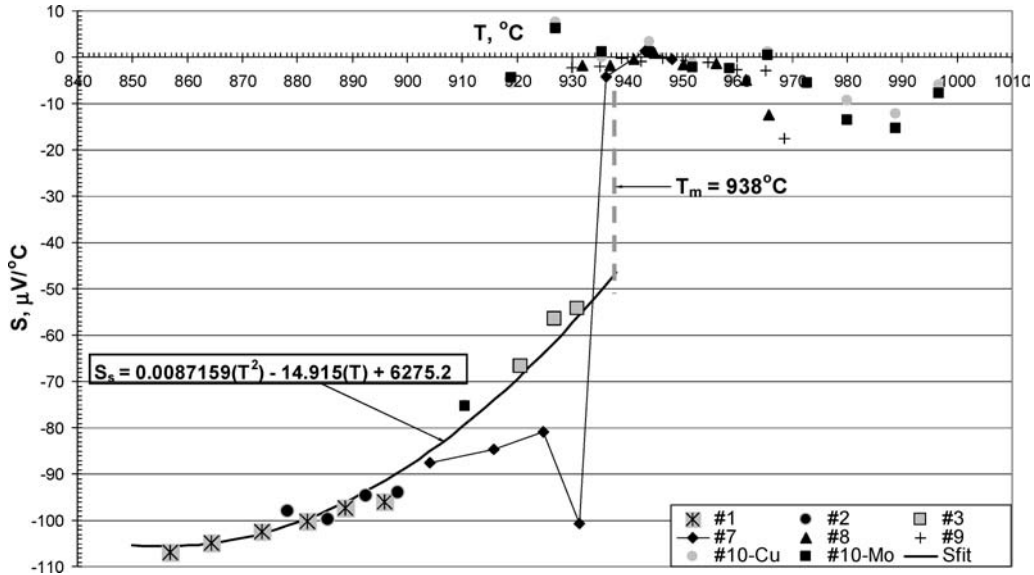


Figure 3 Measured Seebeck coefficient values. Experiments #1, #2, and #3 were conducted with fully solid samples. A second order polynomial shown in the figure fit these data very well. Experiments #7, #8, #9, and #10 were carried out with initially fully liquid samples. A value of $-0.6 \mu\text{V}/^\circ\text{C}$ was obtained between 938 and 960°C, above which the Seebeck coefficient dropped down to about $-18 \mu\text{V}/^\circ\text{C}$. When the cold end of these samples were cooled below the melting point of 938°C, the Seebeck coefficient still stayed around the values representative of the liquid, indicating a melt supercooling. With supercooled (or partially solid) samples, the data near the melting point fell much below those obtained with fully solid samples and later caught up with the data for solid samples, see data points for #7 as an example.

Uncertainty on the Seebeck voltage due to temperature fluctuations at the junctions ($\pm 1^\circ\text{C}$) is of the order $30 \mu\text{V}$ in the solid range and $-0.25 \mu\text{V}$ in the liquid range according to Equation 6, which is the derivation of Equation 4.

$$dE_T = dT_c(S_{\text{Cu-s}}) + dT_h(S_{\text{l-Cu}}) \quad (6)$$

Fig. 3 displays the results of the measurements. For the Seebeck coefficient of the solid germanium, the experiments (#1, #2, and #3) were performed with a completely solid bar by keeping both the hot and cold junction temperatures below the melting point of germanium (938°C). The hot and cold end junction temperatures are given in Table I. In the solid range, the Seebeck coefficient increased from $-107 \mu\text{V}/^\circ\text{C}$ at 857°C to $-54 \mu\text{V}/^\circ\text{C}$ at 931°C. A sudden jump, to around zero, in the Seebeck coefficient was observed when the sample was liquid, marked with a vertical dashed line in Fig. 3. A second order polynomial curve fits the obtained experimental data for the solid quite well as seen in the figure. According to the fit, the Seebeck coefficient of the solid right below the melting point is $-46 \mu\text{V}/^\circ\text{C}$; in contrast, the experimental reading closest to the melting point is obtained at 931°C as $-54 \mu\text{V}/^\circ\text{C}$. Likewise, Vinckel *et al.* [16] reported an experimental value of $-50 \mu\text{V}/^\circ\text{C}$ at the melting point, although they claimed a curve fit value of $-90 \mu\text{V}/^\circ\text{C}$ would be more accurate! Also, Domenicali [15] reported a value of $-70 \mu\text{V}/^\circ\text{C}$ between the solid and liquid germanium.

The Seebeck coefficient of the liquid germanium was measured by having a completely liquid sample (#7, #8, #9, and #10), where both the hot and cold junction temperatures were initially kept above the melting point, as shown in Table I. The data collected in the range 938 to 960°C yielded an average value of $-0.6 \mu\text{V}/^\circ\text{C}$. The Seebeck coefficient for the liquid germanium has been previously reported [13, 15, 16, 22] to be constant

(around $-0.5 \mu\text{V}/^\circ\text{C}$) in the whole liquid range from 938 to 1150°C as also predicted constant by modeling calculations [22–28] due to covalent character of the bonds that persist in the liquid and disappears only at 1727°C [27].

A significant finding in this study was observed in the liquid range from 960 to 1000°C, which appeared as a distinctly visible reduction in the Seebeck coefficient down from an average value of $-0.6 \mu\text{V}/^\circ\text{C}$ to as low as $-18 \mu\text{V}/^\circ\text{C}$. This drop was reproduced by three different experiments (see #8, #9, and #10 in Fig. 3), among which #10 used a second Seebeck voltage probe made of a molybdenum wire together with the copper probe used in all the other experiments. Use of the molybdenum probe was to cross check the copper readings in this high temperature range. A similar finding has been previously reported only by Glazov [21, 33], a value of $-12 \mu\text{V}/^\circ\text{C}$ between 977 and 1030°C, which later increased back to zero above this temperature. Although no explanation has been given for this behavior previously, simulation of liquid germanium [27] that showed a decrease in electrical conductivity above 970°C may be the reason for the decrease in the Seebeck coefficient. In addition, the same simulation work also predicted a decrease in kinematic viscosity around the same temperature as this decrease was also observed experimentally [33]. One other reason for the reduction in the Seebeck coefficient in this temperature range could be the removal of any impurities in the liquid above 960°C [34].

Another notable feature observed in this study was that when the sample was completely liquid at a stable, constant temperature and the cold junction was cooled stepwise from above the melting point to below it in experiments #7–#10, the Seebeck coefficient did not drop down to values characteristic to the solid, see in Fig. 3 the data points obtained in these experiments below the melting point of 938°C. This is due to the melt

supercooling, as also reported by Domenicali [15], although the system was thermally stabilized during each step of the data collection. Moreover, the magnitude of supercooling, as much as $\sim 20^\circ\text{C}$, seems to be larger when cooling from higher melt temperatures, which is in agreement with observations given in [33].

Further cooling of the cold junction of a sample that consisted of a partially superheated melt and partially supercooled melt (or solid) led to a sharp drop in the Seebeck coefficient, which is an indication of solid formation. However, these data points fell much below those obtained with fully solid samples (#1–3). This behavior is represented by the connected data points for sample #7 in Fig. 3, although it was also observed with other samples (#4, #5, #6 in Table I), which were not included in the plot to avoid crowd. However, as cold junction cooled further after this sharp drop, the Seebeck coefficient increased and caught up with the data obtained with completely solid samples. A similar behavior, as scattered data close to melting point, has been also reported by Vinckel [16]. This behavior can be attributed to structural changes in the supercooled liquid. Changes in various material properties in supercooled state have been previously studied and reported [35–37]. Particularly, a study [25] showed that germanium can be supercooled down to 477°C , where the diffusion coefficient drops by a factor of 4 compared to that in the heated liquid, and below 477°C , number of nearest neighbors decreases to 4 and structure is amorphous. In the light of these observations, care should be taken when reporting/using the Seebeck coefficient values obtained with partially solid and partially liquid samples.

4. Conclusions

The Seebeck coefficient of the solid and liquid germanium was measured using the small ΔT method. In the solid, the Seebeck coefficient increased from $-107 \mu\text{V}/^\circ\text{C}$ at 857°C to $-54 \mu\text{V}/^\circ\text{C}$ at 931°C . The data collected in the solid range fit a second order polynomial very nicely. A sudden jump, to around zero, in the Seebeck coefficient was observed when the sample was liquid. While in the liquid from 938 to 960°C , an average value of $-0.6 \mu\text{V}/^\circ\text{C}$ was obtained, the Seebeck coefficient dropped down to about $-18 \mu\text{V}/^\circ\text{C}$ above 960°C due to changes in the electrical conductivity and viscosity. Also, a melt supercooling was observed when cooling the liquid samples, and the magnitude of the supercooling was larger with higher initial melt temperatures.

Acknowledgment

This work was supported by NASA under the grant #450975812, entitled “Morphological Stability of Faceted Interfaces”.

References

1. G. H. RODWAY and J. D. HUNT, *J. Cryst. Growth* **112** (1991) 554.
2. T. J. SEEBECK, *Abh. Konigl. Akad. Wiss.* **265** (1822) 371.

3. N. CUSACK and P. KENDALL, *Proc. Phys. Soc.* **72** (1958) 898.
4. J. J. FAVIER, thesis “Etude expérimentale et théorique de la température d’un front de solidification par application de l’effet thermoélectrique,” CEA (commissariat à l’Energie Atomique), Grenoble, France, 1977.
5. J. ALVAREZ, S. D. PETEVES and G. J. ABBASCHIAN, “Thin Films and Interfaces II,” edited by J.E.E. Beglin *et al.* (North-Holland, NY, 1984) p. 345.
6. G. H. RODWAY and J. D. HUNT, *J. Cryst. Growth* **112** (1991) 563.
7. C. N. LIAO and K. N. TU, *J. Appl. Phys.* **92** (2002) 635.
8. C. N. LIAO, C. CHEN and K. N. TU, *ibid.* **86** (1999) 3204.
9. J. H. KIELY, D. V. MORGAN and D. M. ROWE, *Meas. Sci. Technol.* **5** (1994) 182.
10. S. L. ZHANG, M. OSTLING, H. NORSTROM and T. ARNBORG, *IEEE Trans. Electr. Dev.* **41** (1994) 1414.
11. N. BENAZZI, J. VINCKEL and J. G. GASSER, *J. Non-Cryst. Solids* **201** (1996) 172.
12. A. T. LONCHAKOV, I. M. TSIDILKOVSKI and G. A. MATVEEV, *Sov. Phys. Semicond.* **22** (1988) 529.
13. A. BATH, J. HUGEL and R. KLEIM, *Phys. Stat. Sol. (b)* **128** (1985) 761.
14. A. BATH, J. C. GASSER, J. L. BRETONNET, R. BIANCHIN and R. KLEIM, *J. De Phys.* **C8** (1980) C8-519.
15. C. A. DOMENICALI, *J. Appl. Phys.* **28** (1957) 749.
16. J. VINCKEL, N. BENAZZI, H. HALIM, J. G. GASSER, J. COMERA and P. CONTAMIN, *J. Non-Cryst. Solids* **156–158** (1993) 493.
17. S. FUJITA and H. C. HO, *Mod. Phys. Lett. B* **13** (1999) 689.
18. S. FUJITA, H. C. HO and Y. OKAMURA, *Int. J. Mod. Phys.* **14** (2000) 2231.
19. M. S. ABLOVA and A. P. REGEL, *Sov. Phys. Tech. Phys.* **2** (1957) 2012.
20. B. SIXOU, A. ROUZAUD and J. J. FAVIER, *J. Cryst. Growth* **137** (1994) 605.
21. V. M. GLAZOV, A. A. AIVAZOV and V. A. EVSEEV, *Sov. Phys. Semicond.* **3** (1970) 952.
22. A. MAKRAJDI, J. G. GASSER, J. HUGEL, A. YAZI and M. BESTANDJI, *J. Phys. Cond. Matt.* **11** (1999) 671.
23. M. BESTANDJI, A. MAKRAJDI, H. CHAABA, A. B. MOUSSA and J. G. GASSER, *ibid.* **11** (1999) 8793.
24. H. S. SCHNYDERS and J. B. VAN ZYTVELD, *ibid.* **8** (1996) 10875.
25. N. TAKEUCHI and I. L. GARZON, *Phys. Rev. B* **50** (1994) 8342.
26. G. KRESSE and J. HAFNER, *ibid.* **49** (1994) 14251.
27. R. V. KULKARNI, W. G. AULBUR and D. STROUD, *ibid.* **55** (1997) 6896.
28. V. GODLEVSKY, J. R. CHELIKOWSKI and N. TROULLIER, *ibid.* **52** (1995) 13281.
29. E. BALIKCI, A. DEAL and R. ABBASCHIAN, *J. Cryst. Growth* **262** (2004) 581.
30. *Idem.*, *J. Cryst. Growth Design* **4** (2004) 377.
31. R. B. ROBERTS, *Phil. Magz. B* **43** (1981) 1125.
32. R. B. ROBERTS, F. RIGHINI and R. C. COMPTON, *ibid.* **52** (1985) 1147.
33. V. M. GLAZOV, S. N. CHIZHEVSKAYA and N. N. GLAGOLEVA, “Liquid Semiconductors,” (Plenum Press, NY, 1969), p. 55.
34. P. C. WONG, K. K. LEUNG, C. F. LAU and H. W. KUI, *Scripta Met. Mat.* **32** (1995) 1701.
35. V. I. LADYANOV and L. BELTYUKOV, *JETP Lett.* **71** (2000) 88.
36. K. F. KELTON, A. K. GANGOPADHYAY, G. W. LEE, R. W. HYERS, J. ROGERS, M. B. ROBINSON, T. J. RATHZ, L. HANNET and S. KRISHNAN, presented in the 2002 NASA Materials Science Conference, Huntsville, AL, June 25–26, 2002.
37. S. KRISHNAN, D. L. PRICE, M. L. SABOUNGI and P. C. NORDINE, presented in the 2002 NASA Materials Science Conference, Huntsville, AL, June 25–26, 2002.

Received 10 November 2003

and accepted 29 November 2004